The efficacy of activated protein C in murine endotoxemia is dependent on integrin CD11b

Chunzhang Cao,[1] Yamei Gao,[1] Yang Li,[1] Toni M. Antalis,[1] Francis J. Castellino,[2] and Li Zhang[1]

[1]Center for Vascular and Inflammatory Diseases, Department of Physiology, University of Maryland School of Medicine, Baltimore, Maryland, USA.
[2]W.M. Keck Center for Transgene Research, University of Notre Dame, Notre Dame, Indiana, USA.

Activated protein C (APC), the only FDA-approved biotherapeutic drug for sepsis, possesses anticoagulant, antiinflammatory, and barrier-protective activities. However, the mechanisms underlying its antiinflammatory functions are not well defined. Here, we report that the antiinflammatory activity of APC on macrophages is dependent on integrin CD11b/CD18, but not on endothelial protein C receptor (EPCR). We showed that CD11b/CD18 bound APC within specialized membrane microdomains/lipid rafts and facilitated APC cleavage and activation of protease-activated receptor–1 (PAR1), leading to enhanced production of sphingosine-1-phosphate (S1P) and suppression of the proinflammatory response of activated macrophages. Deletion of the γ-carboxyglutamic acid domain of APC, a region critical for its anticoagulant activity and EPCR-dependent barrier protection, had no effect on its antiinflammatory function. Genetic inactivation of CD11b, PAR1, or sphingosine kinase–1, but not EPCR, abolished the ability of APC to suppress the macrophage inflammatory response in vitro. Using an LPS-induced mouse model of lethal endotoxemia, we showed that APC administration reduced the mortality of wild-type mice, but not CD11b-deficient mice. These data establish what we believe to be a novel mechanism underlying the antiinflammatory activity of APC in the setting of endotoxemia and provide clear evidence that the antiinflammatory function of APC is distinct from its barrier-protective function and anticoagulant activities.

Introduction

As many as 500,000 individuals in the US develop sepsis each year, from a variety of offending pathogens, and as many as half these cases are fatal. Prominent features of the septic response include uncontrolled inflammation and coagulation (1). Numerous clinical trials of antiinflammatory and antithrombotic agents have been aimed at effective treatment of sepsis. They included evaluation of the efficacy of mAbs to the Gram-negative endotoxin LPS or to TNF-α. Other types of interventions were attempted with NOS inhibitor, Fc fusions with soluble TNF receptors (sTNFRs) and IL-1 receptor antagonist (IL-1Ra), and administration of tissue factor pathway inhibitor (TFPI) and antithrombin III. These strategies all failed to achieve statistically significant reduction in the 28-day mortality rate of septic shock patients in phase III clinical trials (2). Surprisingly, activated protein C (APC; Xigris), a natural anticoagulant protein, exhibited effectiveness in severe sepsis patients (3) and has been approved by the FDA as an antisepsis drug. However, the mechanism of its antisepsis activity is not fully understood, and uncertainties regarding its efficacy, safety, and cost effectiveness still persist.

APC is a serine protease derived from its inactive zymogen, protein C (PC). Activation of PC is optimally accomplished on EC surfaces with PC bound to its receptor, endothelial protein C receptor (EPCR), via its γ-carboxyglutamic acid (Gla) domain (4), and the activator, thrombin, bound to EC-resident thrombomodulin (TM; ref. 5). Once activated, APC inhibits both intrinsic and extrinsic coagulation pathways by limited proteolytic cleavages of the procoagulant cofactors, activated coagulation Factor V (FVa) and Factor VIII (FVIIIa), consequently downregulating the conversion of prothrombin to thrombin. In addition to its antithrombotic function, APC exhibits direct vascular barrier protective activity toward ECs by binding to EPCR within the specialized membrane microdomains (i.e., lipid rafts) of the cell membrane and subsequently cross-activating protease activated receptor–1 (PAR1; ref. 6). This cascade initiates a number of intracellular signaling pathways, including upregulation of sphingosine kinase–1 (SphK1) activity and, thus, production of sphingosine-1-phosphate (S1P), leading to activation of signaling via its receptor, S1P1 (7). In addition, other cryoprotective functions of APC have been documented in various cell types, such as attenuation of hypoxia-induced apoptosis of brain ECs by downregulating p53 and blocking caspase-3 activation (8) and of TNF-treated ECs by suppressing the proapoptotic mediator TNF-related apoptosis–inducing ligand (TRAIL; ref. 9). In support of its direct involvement as a barrier protective agent, a mutant of APC, [KKK192-194AAA,RR229-230AA]APC (5A-APC), which exhibits little antithrombotic activity, possesses nearly full barrier-protective activity (10), which suggests that the barrier and cytoprotective functions of APC are independent of its anticoagulant activity.

APC also suppresses leukocyte production of the proinflammatory cytokines IL-1β, IL-6, and IL-12 (11, 12), potentially by inhibiting Wnt5A expression (13); increases the production of antiinflammatory cytokines IL-10 and TGFβ (14); and blocks neutrophil migration in vitro (15). However, the mechanism underlying its antiinflammatory function is poorly understood, particularly in regard to the involvement of its receptor, EPCR (12, 14–18). Here, we report our evidence, using LPS-induced lethal endotoxemia as a model of sepsis in mice, that the efficacy of APC as an effective antiinflammatory agent toward activated macrophages is critically dependent on integrin CD11b/CD18.

Conflict of interest: The authors have declared that no conflict of interest exists.
Citation for this article: *J Clin Invest.* 2010;120(6):1971–1980. doi:10.1172/JCI40380.

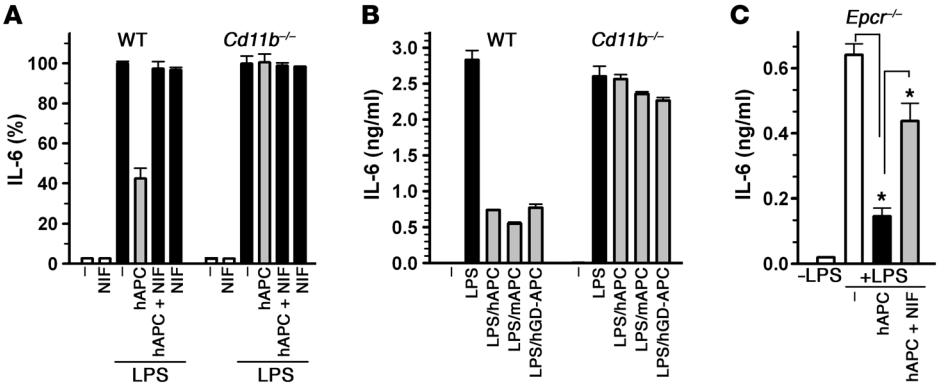

Figure 1

The antiinflammatory function of APC is independent of EPCR, but requires integrin CD11b/CD18. WT, *Cd11b*$^{-/-}$ (**A** and **B**), and *Epcr*$^{-/-}$ (**C**) macrophages, derived by differentiation of BM cells from their corresponding mice, were stimulated by 50 ng/ml LPS in the presence of BSA (as a control) or 0.09 μM hAPC, mAPC, or hGD-APC, with or without NIF (50 nM). Nonstimulated macrophages were used as a control. IL-6 concentration in the conditioned media was determined 20 hours later by ELISA. Data are mean ± SD of 2–3 samples and are representative of 3 independent experiments. *$P < 0.01$.

Results

The antiinflammatory activity of APC on macrophages is dependent on CD11b/CD18, but not on EPCR. As reported by the Recombinant human activated Protein C Worldwide Evaluation in Severe Sepsis (PROWESS) study group, administration of APC in sepsis patients leads to significant reduction in plasma IL-6 concentration (3); however, its underlying mechanism is not fully understood. In light of the uncertainties surrounding the role of EPCR in the antiinflammatory activity of APC (12, 14, 15, 17), we studied APC-mediated suppression of IL-6 production by macrophages in response to LPS stimulation. We used BM-derived macrophages, as they exhibited a high degree of homogeneity compared with peritoneal lavaged cells. We found that treatment of LPS-stimulated macrophages with human APC (hAPC) substantially blocked production of the proinflammatory cytokine IL-6 (Figure 1A), in good agreement with published data (11–15, 17). No significant difference was observed between murine APC (mAPC) and hAPC in their IL-6–suppressive activity with macrophages (Figure 1B). Surprisingly, deletion of the Gla domain of hAPC (hGD-APC), which abrogates its anticoagulant activity and its binding activity toward EPCR (4), did not markedly affect its antiinflammatory activity (Figure 1B). This demonstrated that the ability of APC to suppress IL-6 production on macrophages does not require its anticoagulant activity or its interaction with EPCR. To further investigate a potential role of EPCR in the antiinflammatory function of APC, we prepared macrophages from *Epcr*$^{-/-}$ mice, derived as described previously (19). We found that IL-6 production by LPS-stimulated *Epcr*$^{-/-}$ macrophages, like their WT counterparts, was significantly suppressed by APC (Figure 1C).

To search for other receptors that may support the antiinflammatory activity of APC on leukocytes, we determined whether CD11b/CD18, a heterodimeric integrin receptor highly expressed on leukocytes and known to interact with EPCR via protease 3 (20), is required for APC-mediated suppression of IL-6 production. We found that addition of the CD11b-specific antagonist NIF, which did not affect IL-6 production per se, blocked the IL-6–suppressive activity of APC toward WT and *Epcr*$^{-/-}$ macrophages (Figure 1, A and C). Most importantly, we found that genetic inactivation of CD11b completely abolished the ability of APC to suppress IL-6 production (Figure 1B), demonstrating that CD11b/CD18 is essential to the antiinflammatory function of APC on macrophages.

LDL receptor–related protein 8 (LRP8; also known as apoE receptor 2) was reported to support APC signaling in human monocytic U937 cells by a mechanism independent of both EPCR and PAR1 (16). We found that LRP8 did not play a major role in the antiinflammatory function of APC on primary macrophages because BM-derived macrophages did not express LRP8, based on RT-PCR (Supplemental Figures 1 and 2; supplemental material available online with this article; doi:10.1172/JCI40380DS1), and because receptor-associated protein (RAP), a small antagonist that blocks LRP8-dependent U937 cell adhesion to APC (16), failed to inhibit macrophage adhesion (Figure 2A) or block the IL-6–suppressive activity of APC (Supplemental Figure 2).

APC is a physiological ligand of CD11b/CD18 on macrophages. The observation that EPCR was not required for the antiinflammatory function of APC (Figure 1C) suggested that CD11b/CD18 contributed to the inflammatory-suppressive function of APC by an EPCR-independent mechanism. CD11b/CD18 is an integrin receptor possessing a unique ability to recognize a very wide range of ligands (21). We hypothesized that APC binds to CD11b/CD18 on macrophages and thereby suppresses the proinflammatory response of activated macrophages. To test this hypothesis, we investigated whether APC serves as a physiological ligand of CD11b/CD18 by conducting a series of complementary experiments. First, we found that immobilized APC (Figure 2A) and GD-APC (Supplemental Figure 3) supported strong macrophage adhesion, which was blocked by the CD11b-specific antagonist NIF and the function-blocking mAb M1/70, but not by RAP. Second, genetic inactivation of CD11b blocked macrophage adhesion to immobilized APC (Figure 2A) and GD-APC (Supplemental Figure 3), whereas inactivation of the EPCR gene had no effect (Figure 2A). Third, soluble APC bound macrophages in suspension, which was abrogated by genetic inactivation of CD11b (Figure 2B). Quantification of APC binding by flow cytometry demonstrated that APC bound macrophages in a dose-dependent manner with a 50% effective concentration of 0.4 μM (Figure 2B), an affinity typical for integrin/ligand interactions. Fourth, addition of soluble hAPC and mAPC as well as GD-APC blocked macrophage adhesion to immobilized hAPC (Supplemental Figure 4). Finally, we found that APC was coimmunoprecipitated with CD11b/CD18 in solution (Figure 2C) and that APC and CD11b/CD18 colocalized on the surface of macrophages (Figure 2D).

The antiinflammatory activity of APC is dependent on PAR1 and lipid rafts. PAR1 is critical to the barrier enhancement and cytoprotective functions of APC on vascular ECs (6). To investigate whether antiinflammatory activity of APC on macrophages is also dependent on PAR1, we investigated whether the PAR1-specific antagonist SCH79797 would interfere with the suppressive function of APC

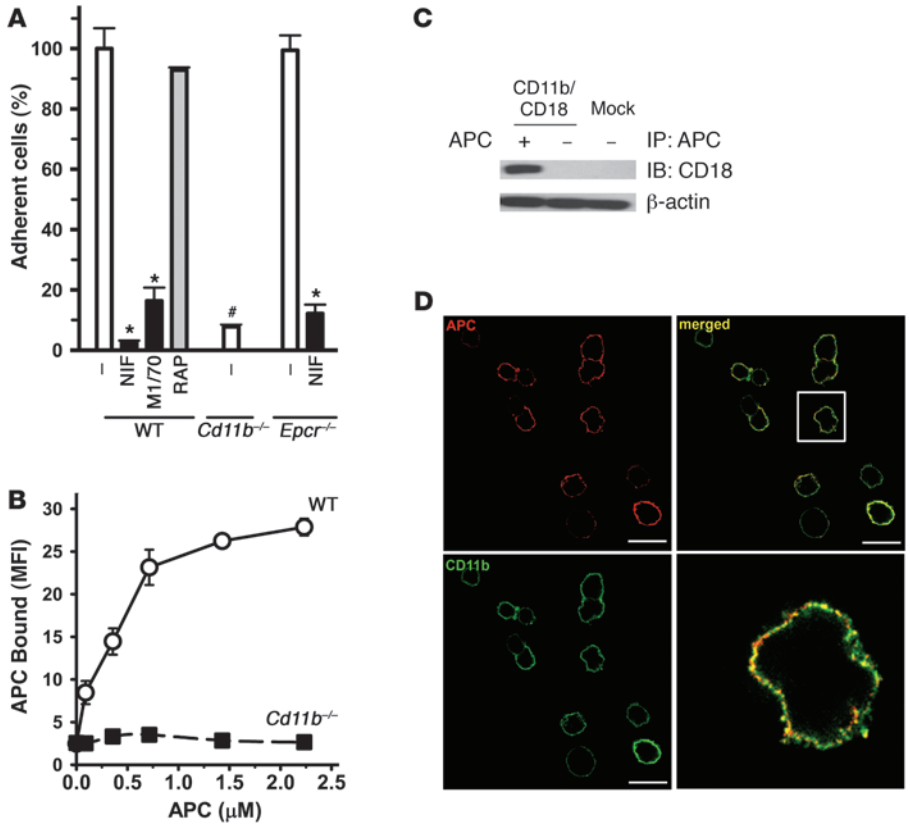

Figure 2

APC is a physiological ligand of CD11b/CD18. (**A**) Cell adhesion. BM-derived macrophages were allowed to adhere to APC in the presence of 10 nM NIF, 20 μg/ml M1/70, or 40 μg/ml RAP. After washing, adherent cells were counted manually under a microscope. The number of adherent WT macrophages in the absence of inhibitors was assigned 100%. **P* < 0.0001 versus unstimulated; #*P* < 0.0005 versus WT. (**B**) Soluble APC binding. APC was incubated with WT or *Cd11b*$^{-/-}$ macrophages in solution. After washing, bound APC was determined by flow cytometry using a goat anti-APC antibody based on MFI. Data are mean ± SD of triplicate samples. (**C**) Coimmunoprecipitation. CD11b/CD18-expressing or mock-transfected HEK293 cells were treated with APC, washed, and then lysed. The cell lysates were immunoprecipitated using a goat anti-APC antibody, and the pulldown materials were separated on 10% SDS-PAGE and probed with rabbit anti-CD18 antibody ARC22 by Western blot. Equal loading was verified by immunostaining the total cell lysates with anti–β-actin antibody. (**D**) Colocalization. BM-derived macrophages were treated with APC and then adhered to poly-lysine–coated coverslips. The cells were stained with mouse anti-CD11b/CD18 mAb M1/70 and a goat anti-APC antibody, followed by Alexa Fluor 488–conjugated anti-rat IgG and Alexa Fluor 568–conjugated anti-goat IgG. Specificity was verified using nonimmune rat and goat IgGs (data not shown). Representative images shown were taken with ×100 objective oil lens with a slice thickness of 2.6 μm; an enlarged view of the boxed region in the merged image is shown at bottom right. Scale bars: 20 μm.

toward LPS-stimulated macrophages. First, we found that BM-derived macrophages expressed PAR1 transcript (Supplemental Figure 5) and antigen (Figure 3C), neither of which was affected by deficiency of CD11b (Supplemental Figure 5). Second, we found that addition of SCH79797 to macrophages in the presence of LPS and APC significantly blocked the IL-6–suppressive activity of APC (Figure 3A; $P = 0.025$). To directly confirm the essential role of PAR1 in this antiinflammatory function of APC, we repeated the above experiments using macrophages prepared from *Par1*$^{-/-}$ mice, which expressed cell surface levels of CD11b similar to those of their WT counterparts (Supplemental Figure 5), and found that APC failed to suppress IL-6 production in the absence of PAR1 (Figure 3B).

The high efficiency of thrombin-mediated PAR1 cleavage is attributed to the presence of a hirudin-like motif within the tethered ligand (22). As APC does not recognize this hirudin-like sequence, it requires EPCR or other cell surface receptors, preferentially within the lipid rafts of the cell membrane, for optimal cleavage of PAR1 (22). To assess whether the antiinflammatory function of APC is similarly dependent on lipid rafts, we treated BM-derived macrophages with methyl-β-cyclodextrin (MβCD), an agent that disrupts the lipid rafts structure, and then stimulated the treated macrophages with LPS in the presence or absence of APC. We found that MβCD treatment abolished the ability of APC to suppress IL-6 production by LPS-stimulated macrophages (Figure 3A).

The ability of APC to cleave PAR1 on the macrophage surface is dependent on CD11b/CD18. The above data demonstrated that the antiinflammatory activity of APC is dependent on CD11b/CD18, PAR1, and lipid rafts, which suggests that CD11b/CD18 on macrophages may serve an equivalent role as EPCR on ECs to facilitate APC cleavage of PAR1. In support of our hypothesis, we found that CD11b/CD18 and PAR1 both resided within the lipid rafts (Figure 3C) and were colocalized on the cell surface (Figure 3D). To directly investigate whether APC cleavage of PAR1 is dependent on CD11b/CD18, we probed PAR1 cleavage using the cleavage-sensitive mAb ATAP2, which recognizes an epitope in the N-terminal region of hPAR1. This unique epitope is not accessible upon PAR1 cleavage (23). We found that incubation of human macrophage THP-1 cells with APC (Figure 4A) or thrombin (Figure 4B) led to a time-dependent reduction in ATAP2 binding to THP-1 cells, showing that both APC and thrombin were capable of cleaving PAR1 on macrophages. Importantly, we found that addition of NIF significantly blocked PAR1 cleavage by APC (Figure 4A), but had no effect on PAR1 cleavage by thrombin (Figure 4B). These results demonstrated that the ability of APC to cleave PAR1 on macrophages requires CD11b/CD18.

APC-mediated production of S1P by activated macrophages requires the presence of CD11b/CD18. APC activation of PAR1 on ECs leads to enhanced SphK1 activity and the production of S1P, a bioactive lipid that enhances EC barrier function (6). Given that S1P also inhibits proinflammatory cytokine production by macrophages via activation of its receptor S1P1 (24), we hypothesized that CD11b/CD18 facilitates the antiinflammatory function of APC

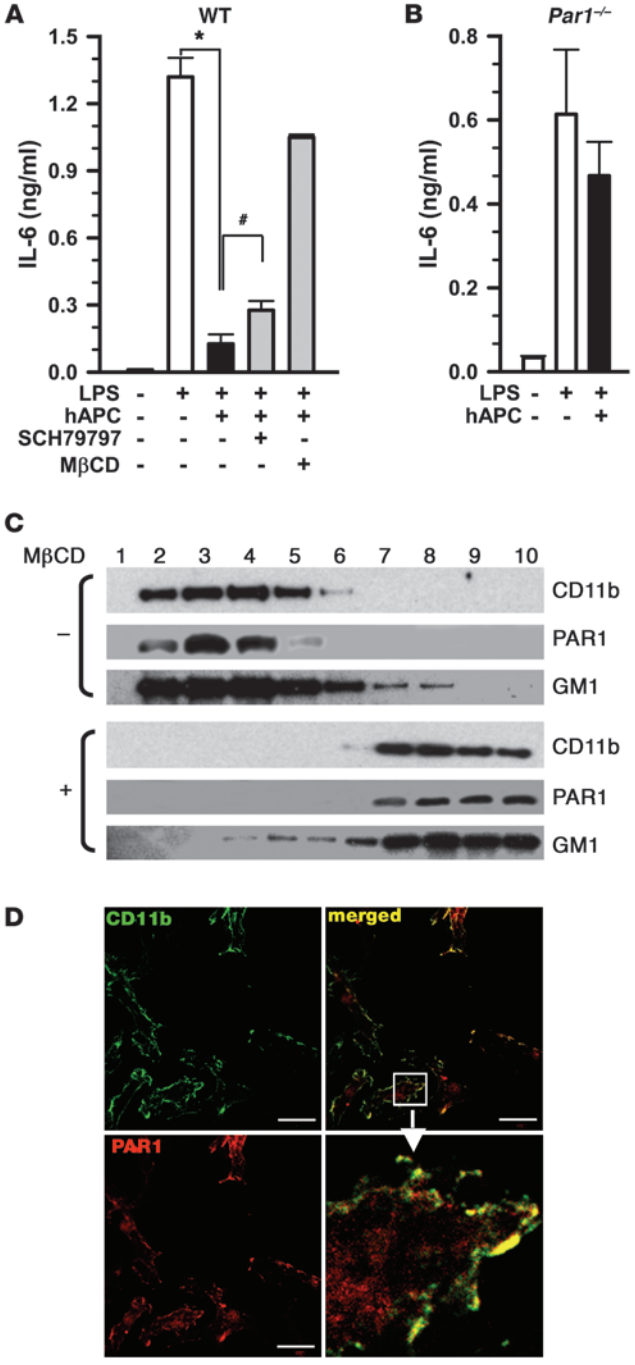

Figure 3
The antiinflammatory function of APC is dependent on PAR1 and lipid rafts. (**A** and **B**) IL-6 production. WT (**A**) or *Par1*$^{-/-}$ (**B**) macrophages were treated with 0.09 μM hAPC in the presence of 0.1 mM SCH79797 or 0.25 mM MβCD and stimulated with LPS. IL-6 concentration in the conditioned media was determined by ELISA (n = 3). *P < 0.0001; #P = 0.029. (**C**) Lipid rafts. Murine macrophage RAW264 cells were treated with or without 0.25 mM MβCD and lysed. Cell lysates were separated by sucrose gradient ultracentrifugation, and the presence of CD11b, PAR1, and GM1 (a marker for lipid rafts) within the different fractions was determined by Western blot. (**D**) Colocalization between CD11b/CD18 and PAR1. BM-derived macrophages were stained with antibodies specific for CD11b (green) and PAR1 (red) and visualized by laser-scanning confocal fluorescence microscopy. Representative images shown were taken with ×100 objective oil lens with a slice thickness of 2.6 μm; an enlarged view of the boxed region in the merged image is shown at bottom right. Scale bars: 20 μm.

on macrophages by enhancing S1P production. In support of our hypothesis, we found that treatment of activated macrophages with APC significantly enhanced S1P production, and this effect was blocked by NIF (Figure 5A). To directly confirm the critical role of CD11b/CD18, but not EPCR, in S1P production, we repeated these experiments using BM-derived macrophages from *Cd11b*$^{-/-}$ and *Epcr*$^{-/-}$ mice. We found that genetic inactivation of CD11b abolished the ability of APC to enhance S1P production, whereas genetic inactivation of EPCR had no effect (Figure 5A). Finally, we found that APC failed to upregulate S1P expression within LPS-stimulated *Sphk1*$^{-/-}$ macrophages, which suggests that SphK1 mediates production of S1P in response to APC.

S1P is capable of suppressing inflammatory activity of Cd11b$^{-/-}$ *macrophages*. If CD11b/CD18 functions to facilitate the antiinflammatory activity of APC by enhancing S1P production, we would anticipate that S1P analogs should be able to directly suppress IL-6 production by *Cd11b*$^{-/-}$ macrophages. Indeed, we found that FTY720 (a S1P analog that activates multiple S1P receptors, including S1P1, S1P3, and S1P4) and SEW2871 (which specifically activates S1P1) significantly blocked IL-6 production by LPS-stimulated WT, *Cd11b*$^{-/-}$, and *Sphk1*$^{-/-}$ macrophages (Figure 5B), demonstrating that S1P1 is involved in the antiinflammatory activity of APC toward macrophages.

It has been reported recently that APC protects TNF-treated ECs from apoptosis by suppressing TRAIL transcription in a PAR1/S1P1-dependent, EPCR-independent mechanism (9). To determine whether the antiinflammatory activity of APC toward macrophages occurs via a similar mechanism, we assessed TRAIL transcription by LPS-stimulated macrophages using quantitative real-time RT-PCR (qRT-PCR). We found that APC only marginally reduced TRAIL expression by WT macrophages, and no reduction was seen with *Cd11b*$^{-/-}$ cells (Figure 5C). It has also been reported that APC blocks macrophage inflammatory response by suppressing Wnt5A expression (13). Indeed, we found that APC treatment of LPS-stimulated macrophages significantly reduced Wnt5A expression (P < 0.05). Importantly, APC failed to suppress Wnt5A expression in the absence of CD11b (Figure 5C).

To investigate if APC and S1P are capable of inhibiting broad inflammatory responses, we stimulated WT and *Cd11b*$^{-/-}$ macrophages with LPS in the presence or absence of APC or FTY720. At 5 hours after administration of these pharmacologic agents, transcript levels of different proinflammatory cytokine genes were assessed by qRT-PCR. We found that FTY720 functioned to suppress proinflammatory cytokine production by WT macrophages in a manner similar to that of APC: both significantly inhibited the transcription of IL-6, IL-12A, NOS2A (iNOS), STAT3, and NF-κB. For *Cd11b*$^{-/-}$ macrophages, FTY720, but not APC, was capable of reducing the transcription of these proinflammatory genes (Figure 5D).

APC suppresses the production of proinflammatory cytokines in WT mice, but not Cd11b$^{-/-}$ *mice, in a mouse model of endotoxemia*. To evaluate whether the ability of APC to stimulate S1P and suppress IL-6 production in vivo was also dependent on CD11b/CD18 under the setting of endotoxemia, WT and *Cd11b*$^{-/-}$ mice were injected i.p. with a single nonlethal dose of LPS, with or without i.v. injection of 10 μg hAPC, mAPC, or hGD-APC. Blood samples were col-

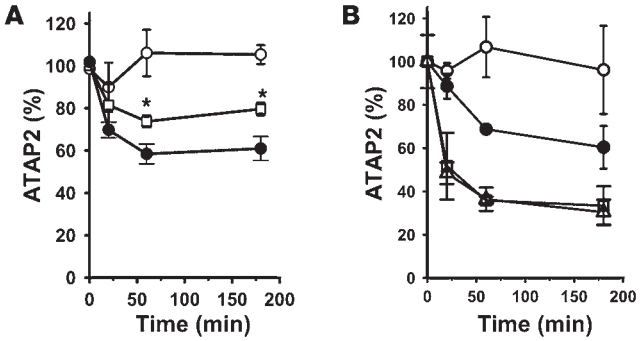

Figure 4
Efficient cleavage of PAR1 by APC but not thrombin is dependent on CD11b/CD18. (**A**) Human macrophage THP-1 cells were treated with PBS (open circles) or 20 nM hAPC with (open squares) or without (filled circles) 10 nM NIF at 37°C. (**B**) THP-1 cells were treated with PBS (open circles), 20 nM hAPC (filled circles), or 1 nM thrombin with (open squares) or without (open triangles) 50 nM NIF at 37°C. At different time points, binding of 0.5 μg/ml ATAP2 to surface PAR1 was determined. The amount of bound ATAP2 at time 0 was assigned 100%. Data are mean ± SD of triplicate experiments. *$P < 0.05$, hAPC versus hAPC plus NIF.

lected from these mice 20 hours later, and plasma concentrations of S1P and IL-6 were measured. Injection of APC significantly increased plasma S1P concentration in WT mice; however, no enhancement was observed in *Cd11b*$^{-/-}$ mice (Figure 6A). Consistent with the higher plasma S1P concentration in WT mice, APC injection significantly lowered the plasma concentration of IL-6 in WT animals, whereas APC injection of *Cd11b*$^{-/-}$ mice did not have a significant effect (Figure 6B). No species difference between hAPC and mAPC was observed with regard to their inflammatory-suppressive activities. Moreover, we found that injection of GD-APC in WT mice, but not *Cd11b*$^{-/-}$ mice, also significantly reduced plasma IL-6 levels (Figure 6B), further demonstrating the lack of involvement of EPCR in this activity.

CD11b/CD18 is critical to the beneficial effect of APC as an antiendotoxemia/sepsis drug. Given the central role of inflammation in the pathogenesis of sepsis (1), we next evaluated whether the ability of APC to protect mice from sepsis-induced mortality also relies on CD11b/CD18. We chose lethal endotoxemia as a mouse model of sepsis, as the other 2 commonly used sepsis models, the bacterial infection model and the cecal ligation and puncture model, also depend on leukocyte-mediated clearance of opsonized bacteria, a process that critically involves CD11b/CD18 (25). Accordingly, WT and *Cd11b*$^{-/-}$ mice were injected i.p. with a single LD_{90} dose of LPS, followed by 2 injections of APC or GD-APC. Administration of either hAPC (Figure 6C) or mAPC (Supplemental Figure 6) significantly protected WT mice, but not *Cd11b*$^{-/-}$ mice, from sepsis-induced death. Moreover, injection of diisopropylfluorophosphate-treated (DFP-treated) GD-APC or Gla domain–deleted hPC (hGD-PC), both of which lacked enzymatic activity, did not significantly reduce sepsis-induced mortality (Figure 6C). Histological analyses of the lungs obtained from these different groups of mice revealed abundant infiltrating leukocytes in LPS-treated WT mice, levels of which were reduced by i.v. injection of APC. In contrast, injection of APC did not significantly reduce leukocyte infiltration in *Cd11b*$^{-/-}$ mice (Figure 6D and Supplemental Figure 9).

Discussion

Sepsis is characterized by disseminated inflammation (termed systemic inflammatory response syndrome; SIRS), enhanced thrombosis, and impaired barrier function, among which the uncontrolled inflammatory response is critical to the initiation and progression of the disease (1). Indeed, clinical studies demonstrate that administration of exogenous APC significantly reduces the IL-6 concentration in the blood and improves overall survival of severely septic patients (3). Here we show, for the first time to our knowledge, that the efficacy of APC as an antiendotoxemia/sepsis drug in vivo is dependent on CD11b/CD18. The mechanism by which APC suppresses IL-6 production and systemic inflammation involves its binding to CD11b/CD18 within lipid rafts on the macrophage surface, which facilitates APC-mediated cleavage and activation of PAR1 and thus increases production of S1P by SphK1. The enhanced S1P suppresses macrophage proinflammatory responses through binding to its receptor S1P1. These data define what we believe to be a novel pathway for APC-mediated antiinflammatory activity toward macrophages that affects mortality in a model of lethal endotoxemia/sepsis.

CD11b/CD18 is an adhesion receptor involved in broad biological functions, including phagocytosis of opsonized particles, cell-mediated cytotoxicity, chemotaxis, and respiratory burst, potentially by recognizing a wide range of ligands (21). Genetic inactivation of CD11b leads to higher mortality after cecal ligation and puncture, primarily as a result of defective clearance of opsonized bacteria by mast cells (25). CD11b/CD18 also supports neutrophil and monocyte adhesion and migration in vitro, although genetic inactivation of CD11b paradoxically enhanced neutrophil and monocyte/macrophage infiltration in vivo (26, 27). In this study, we demonstrated that CD11b/CD18 is also essential to the antiinflammatory function of APC on macrophages. Specifically, we showed that CD11b/CD18 interacted with APC and thereby facilitated its cleavage of PAR1 within lipid rafts of the cell membrane independent of EPCR (Figure 4). Given that soluble EPCR can interact with CD11b/CD18 indirectly via protease 3 (20), our findings do not exclude the possibility that CD11b/CD18 may promote PAR1 activation indirectly via CD11b/CD18–protease 3–soluble EPCR complex. Activation of PAR1 led to enhanced production of S1P by SphK1 (Figure 5A), which in turn suppressed the proinflammatory response of activated macrophages via S1P1 (Figure 5D). S1P is synthesized by 2 sphingosine kinases, SphK1 and SphK2, in a highly compartmentalized manner, where S1P is low in interstitial spaces and high in plasma and lymph tissues (28). Genetic deletion of *Sphk1* alone had only a modest effect on plasma S1P level, due to compensation by SphK2 (29, 30). In fact, FTY720 can be phosphorylated and induce lymphopenia in *Sphk1*$^{-/-}$ mice (29), but not in *Sphk2*$^{-/-}$ mice (30). In a recent study, genetic deletion of both *Sphk1* and *Sphk2*, via conditional gene inactivation, showed an undetectable level of plasma S1P. These mice exhibited basal vascular leak and increased sensitivity to inflammatory challenges, in part due to defective S1P1 activation. This demonstrated that S1P in the blood compartment is required to maintain vascular integrity (28). Our results suggest that although SphK1 is not required for the maintenance of plasma S1P level, it does play a key role

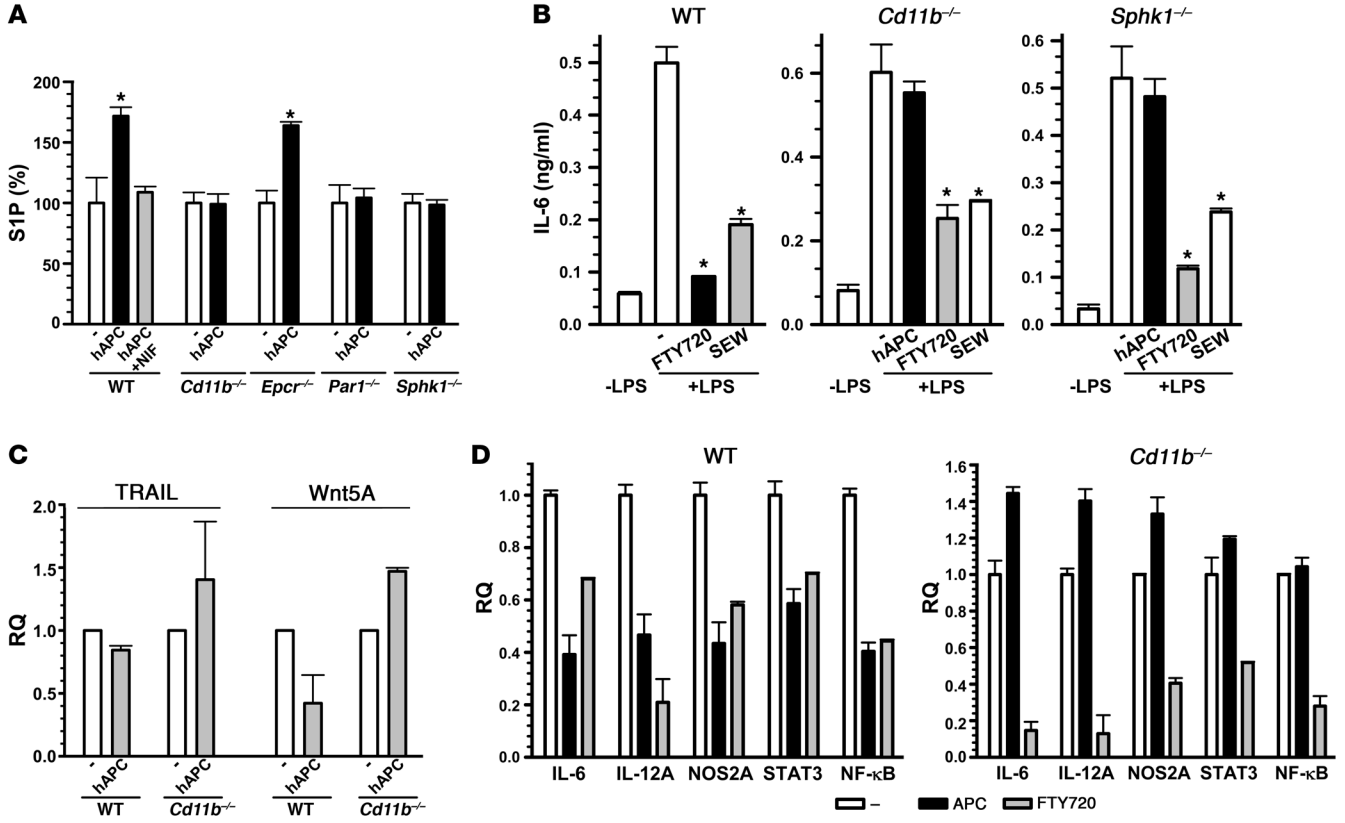

Figure 5

APC-induced S1P production by activated macrophages is dependent on CD11b/CD18 and SphK1. (**A**) BM-derived macrophages from WT, *Cd11b*$^{-/-}$, *Epcr*$^{-/-}$, *Par1*$^{-/-}$, and *Sphk1*$^{-/-}$ mice were stimulated with 10 ng/ml LPS in the presence of PBS, 0.09 μM hAPC, or hAPC plus 10 nM NIF for 5 hours at 37°C. S1P production was quantified by ELISA. The amount of S1P in the absence of hAPC treatment was assigned 100%. **P* < 0.05 versus PBS. (**B**) WT, *Cd11b*$^{-/-}$, and *Sphk1*$^{-/-}$ macrophages were stimulated with LPS in the presence of PBS, 5 μM FTY720, or 5 μM SEW2871 for 20 hours at 37°C. IL-6 in the conditioned media was quantified by ELISA. Nonstimulated macrophages were used as a control. **P* < 0.005 versus PBS. (**C**) WT or *Cd11b*$^{-/-}$ BM-derived macrophages were stimulated with 10 ng/ml LPS in the presence of PBS or 0.09 μM hAPC for 5 hours. Total RNA was prepared, and qRT-PCR was conducted for TRAIL and Wnt5A. All data were normalized to β-actin expression in the same cDNA set. The relative quantity (RQ) values for PBS-treated samples were assigned arbitrarily to 1.0. Relative quantities are mean ± SD of 3 independent experiments. (**D**) WT and *Cd11b*$^{-/-}$ macrophages were stimulated with 10 ng/ml LPS in the presence of PBS, 0.09 μM hAPC, or 5 μM FTY720 for 5 hours, and qRT-PCR was conducted as above using different primer pairs.

in the antiinflammatory response of APC, potentially by increasing S1P levels in both plasma and interstitial space in response to inflammation. Indeed, genetic inactivation of CD11b abolished SphK1-dependent upregulation of S1P production by activated macrophages (Figure 5A). The importance of CD11b/CD18 to the antiinflammatory activity of APC may explain the poor efficacy of the CD18-specific antibody rovelizumab and the CD11b/CD18-specific antagonist NIF to inhibit progression of inflammation in a number of human clinical trials for asthma, inflammatory bowel disease, multiple sclerosis, and rheumatoid arthritis (31).

It has been previously reported that APC blocks neutrophil adhesion and/or migration by inhibiting the functions of the β_1 and β_3 integrins via an RGD sequence (32). However, we found that mAPC, which does not contain a RGD sequence (32), strongly suppressed IL-6 production by LPS-stimulated macrophages (Figure 1B). Moreover, *Cd11b*$^{-/-}$ macrophages expressed β_1 and β_3 integrin levels similar to those of WT macrophages (data not shown), yet failed to adhere to APC (Figure 2, A and B) or respond to APC-mediated suppression (Figures 1 and 5). These data suggested that β_1 and β_3 integrins do not play major roles in APC interaction with macrophages, or in its antiinflammatory functions, in the setting of sepsis. In support of this concept, we found that invasin, a high-affinity ligand of multiple β_1 integrins, such as $\alpha_3\beta_1$, $\alpha_4\beta_1$, $\alpha_5\beta_1$, $\alpha_6\beta_1$, and $\alpha_V\beta_1$ (33, 34), strongly inhibited macrophage adhesion to fibronectin but had no effect on adhesion to APC (Supplemental Figure 7). Moreover, function-blocking antibodies against β_1 or β_3 integrins did not attenuate macrophage adhesion to APC or GD-APC (Supplemental Figure 3), nor did these antibodies reverse APC suppression of IL-6 production in macrophages (Supplemental Figure 2). Blocking the functions of both β_1 and β_3 integrins in mice using an RGD peptide result in only a modest reduction in endotoxemia-induced mortality (32). In addition, because RGD peptides primarily function to inhibit fibrinogen binding to integrin $\alpha_{IIb}\beta_3$, and hence platelet aggregation, the relevance of RGD-dependent protective activity to the antiinflammatory activity of APC is uncertain.

Our study established CD11b/CD18 as the cell surface receptor mediating the antiinflammatory functions of APC toward macrophages. However, the identity and functions of

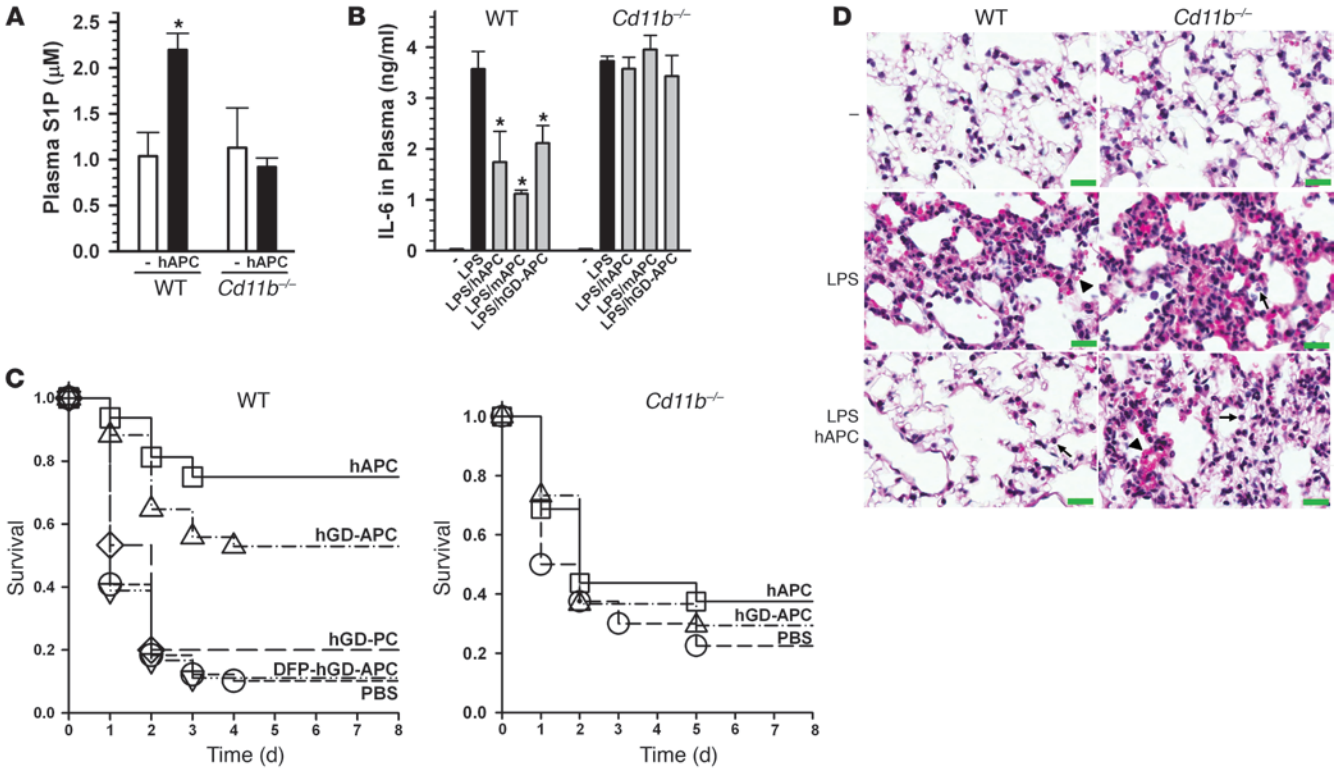

Figure 6

The efficacy of APC as an antiendotoxemia/sepsis drug in vivo is dependent on CD11b/CD18. (**A**) S1P in plasma. WT and *Cd11b*$^{-/-}$ mice (n = 3–4) were injected i.v. with a single dose of 6 μg hAPC or PBS. After 20 minutes, these mice were injected i.p. with 0.8 mg LPS. Blood samples were collected 20 hours later, and concentrations of S1P were determined by ELISA. *P < 0.05 versus PBS. (**B**) IL-6 in plasma. WT and *Cd11b*$^{-/-}$ mice (n = 3) were injected i.p. with 0.8 mg LPS or PBS, followed by i.v. injections with a single dose of 10 μg hAPC, mAPC, hGD-APC, or PBS. Blood samples were collected 20 hours later, and concentrations of IL-6 were determined by ELISA (n = 3–4). *P < 0.05 versus LPS. (**C**) Endotoxemia-induced mortality. WT (n = 15–49) or *Cd11b*$^{-/-}$ (n = 16) mice were injected i.p. with a single LD_{90} dose of LPS, followed by 2 i.v. injections of 10 μg hAPC (squares), 10 μg hGD-APC (triangles), 10 μg hGD-PC (diamonds),10 μg DFP-hGD-APC (inverted triangles), or PBS (circles) at 20 minutes and 8 hours after LPS challenge. Survival was determined over a period of 14 days and shown in Kaplan-Meier plots. Differences versus PBS were determined by log-rank test for WT (P < 0.0001, hAPC and hGD-APC; P = 0.522, hGD-PC; P = 0.960, DFP-hGD-APC) and *Cd11b*$^{-/-}$ (P = 0.585, hAPC; P = 0.497, hGD-APC) mice. (**D**) Histology. WT and *Cd11b*$^{-/-}$ mice were injected i.p. with LPS, followed by i.v. injection of 10 μg hAPC or PBS. Lungs were harvested 20 hours after LPS injection, fixed, and stained with H&E. Images shown are representative of 3 mice. Arrows denote neutrophils; arrowheads denote red blood cells. Scale bars: 20 μm.

intracellular effector molecules downstream of CD11b/CD18 that facilitate the antiinflammatory functions of APC are still unclear. Recently, 2 intracellular proteins, TRAIL and Wnt5A, have been identified as the putative targets of the APC-mediated inhibitory pathway. Specifically, it has been reported that APC blocks the apoptosis of TNF-treated ECs by suppressing TRAIL transcription by a PAR1/S1P1-dependent but EPCR-independent mechanism (9). In addition, it has been demonstrated that APC suppresses inflammation by inhibiting Wnt5A transcription (13). We found that APC inhibition of TRAIL and Wnt5A transcription was dependent on CD11b/CD18 (Figure 5C), suggesting that CD11b/CD18 could be the missing link between APC and its downstream effector molecules in the antiinflammatory pathway.

EPCR is a PC receptor originally identified for its ability to support PC activation (4). More recently, EPCR has been shown to play critical cytoprotective roles in the enhancement of vascular EC barriers (6, 35) and the protection of neuronal cells (8). Several studies suggest that EPCR may play a similar role in the antiinflammatory function of APC on leukocytes, based primarily on studies using function-blocking antibodies (12, 15). However, unlike ECs, macrophages express very low levels of EPCR; consequently, the involvement of EPCR in the antiinflammatory function of APC remains controversial (12, 14, 15, 17). We found that GD-APC, which lacks anticoagulant activity (36), supported CD11b/CD18-dependent macrophage adhesion (Supplemental Figure 3), suppressed IL-6 production both in vitro (Figure 1A) and in vivo (Figure 1B), and protected mice from sepsis-induced mortality (Figure 6C). These findings suggest that the antiinflammatory function of APC is largely independent of its ability to suppress thrombin generation and/or fibrin formation. In addition, since GD-APC does not interact with EPCR (4), these data strongly support our hypothesis that EPCR is not required for the antiinflammatory activity of APC toward macrophages. Indeed, we found that genetic inactivation of EPCR did not have a significant effect on the ability of APC to suppress macrophage production of IL-6 (Figure 1C). In strong support of our finding, it was previously reported that hematopoietic cell–specific EPCR deficiency did not affect host inflammatory response to LPS challenge in vivo (17).

Furthermore, the APC mutant E149A, which exhibits higher anticoagulant activity, normal binding to EPCR, and normal EPCR-dependent PAR1 cleavage on ECs, fails to suppress IL-6 production by LPS-stimulated U937 cells (37).

The timing and duration of APC administration in mice appears to have a major impact on its in vivo function (compare Figure 6B and Supplemental Figure 10). Different suppressive activities toward IL-6 production were observed in vivo when a single dose of GD-APC was administered 50 minutes apart — 30 minutes before (Supplemental Figure 10) and 20 minutes after (Figure 6B) LPS challenge. The mechanism underlying this differential activity is currently unknown and could be due to the short half-life of APC in blood circulation, which ranges from 10 to 25 minutes (38–40), thus resulting in different effective APC concentrations during the peak of endotoxemia.

We found that GD-APC, injected twice at 20 minutes and 8 hours after LPS challenge per a late intervention regimen described by Kerschen et al. (10, 41), led to significant suppression of plasma IL-6 levels at 20 hours after LPS challenge (Supplemental Figure 10) and protection of endotoxemic mice (Figure 6C), suggesting that EPCR-mediated barrier protection may play a less important role if proinflammatory cytokine burst is dampened over time. In support of our observation, Kerschen et al. reported that 2 consecutive injections of 5A-APC at 3 and 10 hours after onset of sepsis provided significantly better protection than a single administration of 5A-APC prior to endotoxin challenge (10, 41). Nevertheless, intact APC exhibited better protection than GD-APC, even using this late intervention regimen (Figure 6C), which suggests that optimal protection by APC of mice from sepsis-induced death requires simultaneous engagement of multiple pathways, among them EPCR/PAR1-dependent barrier protection for ECs and CD11b/PAR1-dependent antiinflammatory activity for macrophages.

In summary, we have identified a mechanism underlying the antiinflammatory activity of APC on macrophages. We showed that the broad inhibitory activity of APC toward macrophage pro-inflammatory responses was dependent on the integrin CD11b/CD18. Importantly, our studies reveal that the presence of CD11b/CD18 on macrophages is critical for the efficacy of APC as an antiendotoxemia/sepsis drug in vivo, which indicates that CD11b/CD18 antagonist therapies would be detrimental in combination with APC. These data provide insight into antiinflammatory activities of APC that are distinct from its barrier-protective function and anticoagulant activities.

Methods

Mice. WT, *Cd11b*$^{-/-}$, *Par1*$^{-/-}$, *Sphk1*$^{-/-}$, and *Epcr*$^{-/-}$ mice were all in the C57BL/6J background and used at 8–13 weeks of age (20–22 g). WT mice were purchased from the National Cancer Institute. *Cd11b*$^{-/-}$ mice were provided by C.M. Ballantyne (Baylor College of Medicine, Houston, Texas, USA), and have been backcrossed to the C57BL/6J background for more than 10 generations. *Par1*$^{-/-}$ mice were provided by S. Coughlin (UCSF, San Francisco, California, USA). *Epcr*$^{lox/lox}$ mice were obtained from C. Esmon (Oklahoma Medical Research Foundation, Oklahoma City, Oklahoma, USA). Meox2-Cre mice, used to derive *Epcr*$^{-/-}$ mice from *Epcr*$^{lox/lox}$ mice, were purchased from the Jackson Laboratory. *Sphk1*$^{-/-}$ mice, used for BM isolation, were from R.L. Proia (National Institute of Diabetes and Digestive and Kidney Diseases, NIH, Bethesda, Maryland, USA). All mice were housed in a pathogen-free facility, and all procedures were performed in accordance with University of Maryland Institutional Animal Care and Use Committee approval.

Antibodies and reagents. mAb F4/80 was from Serotec; mAb M1/70 for CD11b/CD18, mAb MFR5 for integrin β_1, and mAb 2C9.G2 for integrin β_3 were from BD Biosciences — Pharmingen. NIF was provided by E. Plow (Cleveland Clinic Foundation, Cleveland, Ohio, USA; ref. 42). hAPC, hGD-APC, hGD-PC, and goat anti-hPC antibody were from Enzyme Research Laboratories. mAPC was provided by J.H. Griffin (Scripps Research Institute, La Jolla, California, USA). mGD-APC was prepared by chymotrypsin digestion of mAPC, based on previously published methods (36). All experiments were performed using hAPC unless specified otherwise. CD11b/CD18-expressing HEK293 cells and mock-transfected HEK293 cells were generated previously (42). Rabbit polyclonal anti-CD18 cytoplasmic tail antibody ARC22 was prepared as described previously (43). Mannose-binding protein–invasin was provided by J.M. Leong (University of Massachusetts Medical School, Worcester, Massachusetts, USA; ref. 34). The PAR1 antagonist SCH79797 and the EGFR tyrosine kinase inhibitor PP3 were obtained from Tocris Bioscience; S1P1 agonists FTY720 and SEW2871 were from Cayman Chemical. Rabbit anti-PAR1 polyclonal antibody H-111 and the cleavage-sensitive mouse anti-hPAR1 mAb ATAP2 were obtained from Santa Cruz Biotechnology.

Preparation of primary macrophages from BM. BM was flushed from the femur and tibia with DMEM medium and dispersed into single-cell suspension. After lysis of red blood cells with ammonium chloride (8.3 g/l in 10 mM Tris-HCl, pH7.4), BM cells were plated in 10-cm tissue culture Petri dishes in DMEM with 10% FBS and incubated in a humidified incubator with 5% CO_2 at 37°C for 2–4 hours. Suspension cells were collected and cultured in 10-cm Petri dishes at a density of 2×10^5 cells/ml in DMEM with 10% FBS and 10% L929 cell-conditioned medium at 37°C and 5% CO_2 for 7 days. The maturity and purity of the differentiated macrophages were verified by flow cytometry based on their positive staining for F4/80 and M1/70 and negative staining for CD11c as well as by morphological examination of Hema3-stained (Fisher Scientific) Cytospin (Shandon) smears.

Determination of IL-6 and S1P by ELISA. BM-derived macrophages (5×10^5) were switched to serum-free DMEM and stimulated with 50 ng/ml LPS in the absence or presence of 0.09 μM hAPC with or without additional inhibitors for 5 (for S1P) or 20 (for IL-6) hours. To determine S1P production, macrophages were lysed with PIPES buffer, pH 7.4 (20 mM PIPES, 150 mM NaCl, 1 mM EGTA, 1% Triton X-100, 1.5 mM $MgCl_2$, 0.1% SDS, and protease inhibitor cocktail tablet). The concentration of S1P in the cell lysate was determined using the Echelon S1P competitive ELISA according to the manufacturer's instructions (Echelon Biosciences Inc). The concentration of IL-6 in the culture supernatants was determined by ELISA according to the manufacturer's instructions (BD Biosciences — Pharmingen).

Determination of surface PAR1 cleavage using ATAP2. Cleavage of surface PAR1 was monitored using the conformation-sensitive PAR1-specific mAb ATAP2, essentially as described previously (23). Human macrophage-like THP-1 cells were cultured on poly-lysine–coated 96-well plates. Cells were preincubated with or without 10 nM NIF for 10 minutes, and then treated with PBS, 20 nM APC, or 1 nM thrombin for different amount of time at 37°C. The treated THP-1 cells were fixed with 2% PFA, blocked with 2% BSA, and probed with 0.5 μg/ml mouse anti-hPAR1 antibody (ATAP2) for 30 minutes. After washing, bound ATAP2 was quantified using HRP-conjugated anti-mouse secondary antibody and the HRP substrate tetramethylbenzidine, measuring absorbance at 450 nm.

Ligand binding study. Cell adhesion assays were performed as described previously (44). APC (20 μg/ml) was coated at the center of each well of a 24-well non–tissue culture polystyrene plate. The coated plates were blocked with 300 μl 0.05% polyvinylpyrrolidone (Sigma-Aldrich) and then 1% BSA in Dulbecco PBS. A total of 2×10^6 BM-derived macrophages

(WT, *Cd11b*$^{-/-}$, or *Epcr*$^{-/-}$) or CD11b/CD18-expressing or mock-transfected HEK293 cells in HBSS plus 1 mM Ca^{2+} and 1 mM Mg^{2+}, in the presence or absence of NIF (10 nM), M1/70 (20 μg/ml), MFR5 (20 μg/ml), 2C9.G2 (20 μg/ml), RAP (40 μg/ml), or EDTA (5 mM), were added to each well and incubated at 37°C for 20 minutes (for HEK293 cells) or 10 minutes (for macrophages). The unbound cells were removed by 3 washes with PBS. Adherent cells were counted manually under a microscope and then by staining with 0.5% Crystal Violet (Sigma-Aldrich), measuring the absorbance of the cell lysates at 570 nm.

For soluble binding to CD11b/CD18, graded concentrations of APC were incubated with macrophages or transfected human 293 cells in HBSS plus 1 mM Ca^{2+} and 1 mM Mg^{2+} at 4°C for 60 minutes, followed by 3 washes with PBS. Bound APC was detected by flow cytometry using goat anti-hPC and FITC-conjugated rabbit anti-goat secondary antibody, using FACScan (BD Biosciences), counting 10,000 events. MFI was quantified using FACScan.

Coimmunoprecipitation experiments were conducted based on our previously published method (45). CD11b/CD18-expressing or mock-transfected HEK293 cells were treated with APC, washed, and then lysed. The cell lysates were immunoprecipitated using a goat anti-APC antibody, and the immunoprecipitates were separated by 10% SDS-PAGE and probed with the rabbit anti-CD18 antibody ARC22 by Western blotting (44). Equal loading was verified by immunostaining of the total cell lysates with anti–β-actin or anti-CD18 antibody.

Separation of lipid rafts by sucrose gradient ultracentrifugation. Preparation of lipid rafts was accomplished as previously described (43). Murine macrophage-like RAW264 cells were grown to 90% confluence in 150 mm Petri-dishes. After switching to fresh serum-free DMEM medium, the cells were treated with 0.25 mM MβCD at 37°C for 2 hours. After washing with ice-cold PBS, cells were lysed with 2-[morpholino]ethanesulfonic acid–buffered saline (MBS), pH 6.5, containing 1% Triton X-100, 5 mM EDTA, and protease inhibitor cocktail tablet. The lysate was adjusted to 40% sucrose by the addition of an equal volume of 80% sucrose in MBS and put at the bottom of an ultracentrifuge tube. 3 solutions of 30%, 15%, and 5% sucrose were laid sequentially on the top of the 40% sucrose solution. After ultracentrifugation at 116,000 *g* with a Beckman SW Ti55 rotor for 20 hours, 10 0.5-ml fractions were collected from the top of the tubes, and a portion of each fraction was loaded on SDS-PAGE, transferred to PVDF membranes, and subjected to Western blot with their corresponding primary and secondary antibodies.

Analysis of gene expression by qRT-PCR. qRT-PCR was used to evaluate inflammatory responses of LPS-stimulated macrophages. BM-derived macrophages were preincubated with or without APC for 20 minutes, followed by stimulation with 10 ng/ml LPS for 5 hours. Total RNA was extracted using Absolutely RNA miniprep kit (Stratagene) according to the manufacturer's instructions. 1 μg of total RNA was used for cDNA synthesis using Superscript II and random hexamers (Invitrogen). qRT-PCR was performed on an ABI Prism 7500 HT Sequence Detections System (Applied Biosystems), using their corresponding primers (Supplemental Table 1). The PCR reaction was done in 25 μl solution containing 12.5 μl SYBR Green PCR Master Mix, 10 ng cDNA, and 400 nM of each primer, with the following settings: activation of the AmpliTaq Gold Polymerase at 95°C for 10 minutes, 40 cycles of 95°C for 15 seconds and 60°C for 1 minute. The melting curve was analyzed using the ABI software and quantification of gene expression was done based on the $2^{-\Delta\Delta Ct}$ method (RQ Manager 1.4). Each experiment was run in duplicate. All data were normalized to β-actin expression in the same cDNA set.

Confocal laser scanning fluorescence microscopy. Colocalization between APC and CD11b/CD18 was determined by confocal fluorescence microscopy based on our previously published method (45). BM-derived macrophages were incubated with APC at 4°C for 1 hour and allowed to adhere to poly-lysine–coated coverslips. The cells were washed with PBS and fixed with 4% PFA in PBS for 30 minutes at room temperature. After blocking with 5% BSA in PBS at room temperature for 30 minutes, cells were incubated with 10 μg/ml goat anti-APC antibody and 20 μg/ml rat anti-CD11b/CD18 mAb (M1/70) in 1% BSA in PBS at room temperature for 60 minutes. After washing, these different coverslips were incubated with Alexa 488–conjugated rabbit anti-rat IgG and Alexa 568–conjugated rabbit anti-goat IgG (Invitrogen). Similar procedures were used for colocalization between CD11b/CD18 and PAR1, except that BM-derived macrophages were cultured directly on 8-well chamber slides, and 10 μg/ml rabbit anti-PAR1 antibody (H-111; Cell Signaling) was used for staining. After washing, these different slides were incubated with Alexa 488–conjugated goat anti–rat IgG and Alexa 568–conjugated goat anti-rabbit IgG (Invitrogen). Nonimmune rabbit, goat, or rat IgGs were used as specificity controls. The stained macrophages were analyzed using a Bio-Rad Radiance 2000 Confocal Laser Scanning Fluorescence Microscope System equipped with a Nikon Eclipse E800 Upright light microscope. The images were collected using ×100 oil objectives with a slice thickness of 2.6 μm.

Mouse model of lethal endotoxemia. A mouse model of lethal endotoxemia was performed based on the method of Kerschen et al. (10, 41), with minor modifications. Endotoxemia was induced by i.p. injection of a single LD_{90} dose of LPS (*Escherichia coli*; Sigma-Aldrich). hAPC and mAPC, GD-APC, DFP-treated GD-APC, and hGD-PC (10 μg/mouse) or PBS vehicle was administered to WT or *Cd11b*$^{-/-}$ mice via the tail vein at 20 minutes and 8 hours after LPS challenge. Survival of these mice was observed for 14 days. Statistical analysis of animal mortality was done using the log-rank test of the Kaplan-Meier Survival Analysis. To measure plasma concentrations of IL-6 and S1P, mice were injected with LPS and euthanized after 16–20 hours. Blood was collected by retroorbital bleeding into heparin-coated capillaries. Mice were then perfused first with saline and then with 1% PFA in PBS, and lungs were prepared for paraffin-embedded sections. Plasma concentrations of IL-6 and S1P were determined by ELISA as described above. H&E staining was conducted on 5-μm-thick paraffin-embedded sections, and the number of infiltrating leukocytes was determined using NIH ImageJ by counting 5 randomly selected view fields per section.

Statistics. Figures are representative of at least 3 independent experiments. Statistical analyses were performed using 2-tailed Student's *t* test, and the log-rank test of the Kaplan-Meier survival analysis was used to compare the mortality of WT and *Cd11b*$^{-/-}$ mice (Systat Software Inc.). *P* values less than 0.05 were considered significant.

Acknowledgments

We thank Wenji Piao and Elizabeth P. Smith for technical assistance. This work was supported in part by grants from the NHLBI, NIH (HL054710 to L. Zhang and HL073750 to F.J. Castellino), and the American Heart Association (0865073E to C. Cao).

Received for publication July 2, 2009, and accepted in revised form March 17, 2010.

Address correspondence to: Li Zhang, University of Maryland, School of Medicine, 800 W. Baltimore Street, Baltimore, Maryland 21201, USA. Phone: 410.706.8040; Fax: 410.706.8121; E-mail: lizhang@som.umaryland.edu.

Yang Li's present address is: National Eye Institute, NIH, Rockville, Maryland, USA.

1. Buras JA, Holzmann B, Sitkovsky M. Animal models of sepsis: setting the stage. *Nat Rev Drug Discov*. 2005;4(10):854–865.
2. Dyson A, Singer M. Animal models of sepsis: why does preclinical efficacy fail to translate to the clinical setting? *Crit Care Med*. 2009;37(1 suppl):S30–S37.
3. Bernard GR, et al. Efficacy and safety of recombinant human activated protein C for severe sepsis. *N Engl J Med*. 2001;344(10):699–709.
4. Fukudome K, Esmon CT. Identification, cloning, and regulation of a novel endothelial cell protein C/activated protein C receptor. *J Biol Chem*. 1994; 269(42):26486–26491.
5. Esmon CT, Esmon NL, Harris KW. Complex formation between thrombin and thrombomodulin inhibits both thrombin-catalyzed fibrin formation and factor V activation. *J Biol Chem*. 1982; 257(14):7944–7947.
6. Riewald M, Petrovan RJ, Donner A, Mueller BM, Ruf W. Activation of endothelial cell protease activated receptor 1 by the protein C pathway. *Science*. 2002;296(5574):1880–1882.
7. Tauseef M, et al. Activation of sphingosine kinase-1 reverses the increase in lung vascular permeability through sphingosine-1-phosphate receptor signaling in endothelial cells. *Circ Res*. 2008;103(10):1164–1172.
8. Cheng T, et al. Activated protein C blocks p53-mediated apoptosis in ischemic human brain endothelium and is neuroprotective. *Nat Med*. 2003;9(3):338–342.
9. O'Brien LA, et al. Activated protein C decreases tumor necrosis factor related apoptosis-inducing ligand by an EPCR- independent mechanism involving Egr-1/Erk-1/2 activation. *Arterioscler Thromb Vasc Biol*. 2007;27(12):2634–2641.
10. Kerschen EJ, et al. Endotoxemia and sepsis mortality reduction by non-anticoagulant activated protein C. *J Exp Med*. 2007;204(10):2439–2448.
11. Grey ST, Tsuchida A, Hau H, Orthner CL, Salem HH, Hancock WW. Selective inhibitory effects of the anticoagulant activated protein C on the responses of human mononuclear phagocytes to LPS, IFN-gamma, or phorbol ester. *J Immunol*. 1994; 153(8):3664–3672.
12. Stephenson DA, Toltl LJ, Beaudin S, Liaw PC. Modulation of monocyte function by activated protein C, a natural anticoagulant. *J Immunol*. 2006;177(4):2115–2122.
13. Pereira C, Schaer DJ, Bachli EB, Kurrer MO, Schoedon G. Wnt5A/CaMKII signaling contributes to the inflammatory response of macrophages and is a target for the antiinflammatory action of activated protein C and interleukin-10. *Arterioscler Thromb Vasc Biol*. 2008;28(3):504–510.
14. Toltl LJ, Beaudin S, Liaw PC, Canadian Critical Care Translational Biology Group. Activated protein C up-regulates IL-10 and inhibits tissue factor in blood monocytes. *J Immunol*. 2008;181(3):2165–2173.
15. Sturn DH, Kaneider NC, Feistritzer C, Djanani A, Fukudome K, Wiedermann CJ. Expression and function of the endothelial protein C receptor in human neutrophils. *Blood*. 2003;102(4):1499–1505.
16. Yang XV, et al. Activated protein C ligation of ApoER2 (LRP8) causes Dab1-dependent signaling in U937 cells. *Proc Natl Acad Sci U S A*. 2009; 106(1):274–279.
17. Zheng X, et al. Non-hematopoietic EPCR regulates the coagulation and inflammatory responses during endotoxemia. *J Thromb Haemost*. 2007; 5(7):1394–1400.
18. Feistritzer C, Mosheimer BA, Sturn DH, Riewald M, Patsch JR, Wiedermann CJ. Endothelial protein C receptor-dependent inhibition of migration of human lymphocytes by protein C involves epidermal growth factor receptor. *J Immunol*. 2006; 176(2):1019–1025.
19. Li W, et al. Extraembryonic expression of EPCR is essential for embryonic viability. *Blood*. 2005; 106(8):2716–2722.
20. Kurosawa S, Esmon CT, Stearns-Kurosawa DJ. The soluble endothelial protein C receptor binds to activated neutrophils: involvement of proteinase-3 and CD11b/CD18. *J Immunol*. 2000;165(8):4697–4703.
21. Li Z. The alphaMbeta2 integrin and its role in neutrophil function. *Cell Res*. 1999;9(3):171–178.
22. Bae JS, Yang L, Rezaie AR. Lipid raft localization regulates the cleavage specificity of protease activated receptor 1 in endothelial cells. *J Thromb Haemost*. 2008;6(6):954–961.
23. Schuepbach RA, Feistritzer C, Brass LF, Riewald M. Activated protein C-cleaved protease activated receptor-1 is retained on the endothelial cell surface even in the presence of thrombin. *Blood*. 2008; 111(5):2667–2673.
24. Hughes JE, Srinivasan S, Lynch KR, Proia RL, Ferdek P, Hedrick CC. Sphingosine-1-phosphate induces an antiinflammatory phenotype in macrophages. *Circ Res*. 2008;102(8):950–958.
25. Rosenkranz A, et al. Impaired mast cell development and innate immunity in Mac-1 (CD11b/CD18, CR3)-deficient mice. *J Immunol*. 1998; 161(12):6463–6467.
26. Cao C, Lawrence DA, Strickland DK, Zhang L. A specific role of integrin Mac-1 in accelerated macrophage efflux to the lymphatics. *Blood*. 2005;106(9):3234–3241.
27. Coxon A, et al. A novel role for the beta 2 integrin CD11b/CD18 in neutrophil apoptosis: a homeostatic mechanism in inflammation. *Immunity*. 1996; 5(6):653–666.
28. Camerer E, et al. Sphingosine-1-phosphate in the plasma compartment regulates basal and inflammation-induced vascular leak in mice. *J Clin Invest*. 2009;119(7):1871–1879.
29. Allende ML, et al. Mice deficient in sphingosine kinase 1 are rendered lymphopenic by FTY720. *J Biol Chem*. 2004;279(50):52487–52492.
30. Zemann B, et al. Sphingosine kinase type 2 is essential for lymphopenia induced by the immunomodulatory drug FTY720. *Blood*. 2006;107(4):1454–1458.
31. Yonekawa K, Harlan JM. Targeting leukocyte integrins in human diseases. *J Leukoc Biol*. 2005; 77(2):129–140.
32. Elphick GF, et al. Recombinant human activated protein C inhibits integrin-mediated neutrophil migration. *Blood*. 2009;113(17):4078–4085.
33. Hamburger ZA, Brown MS, Isberg RR, Bjorkman PJ. Crystal structure of invasin: a bacterial integrin-binding protein. *Science*. 1999;286(5438):291–295.
34. Leong JM, Morrissey PE, Marra A, Isberg RR. An aspartate residue of the Yersinia pseudotuberculosis invasin protein that is critical for integrin binding. *EMBO J*. 1995;14(3):422–431.
35. Mosnier LO, Zlokovic BV, Griffin JH. The cytoprotective protein C pathway. *Blood*. 2007; 109(8):3161–3172.
36. Esmon NL, DeBault LE, Esmon CT. Proteolytic formation and properties of gamma-carboxyglutamic acid-domainless protein C. *J Biol Chem*. 1983;258(9):5548–5553.
37. Mosnier LO, et al. Hyperantithrombotic, noncytoprotective Glu149Ala-activated protein C mutant. *Blood*. 2009;113(23):5970–5978.
38. Zhong Z, et al. Activated protein C therapy slows ALS-like disease in mice by transcriptionally inhibiting SOD1 in motor neurons and microglia cells. *J Clin Invest*. 2009;119(11):3437–3449.
39. Berg DT, et al. Engineering the proteolytic specificity of activated protein C improves its pharmacological properties. *Proc Natl Acad Sci U S A*. 2003; 100(8):4423–4428.
40. Gruber A, et al. Inhibition of thrombus formation by activated recombinant protein C in a primate model of arterial thrombosis. *Circulation*. 1990;82(2):578–585.
41. Weiler H, Kerschen E. Modulation of sepsis outcome with variants of activated protein C. *J Thromb Haemost*. 2009;7(suppl 1):127–131.
42. Zhang L, Plow EF. Overlapping, but not identical, sites are involved in the recognition of C3bi, neutrophil inhibitory factor, and adhesive ligands by the alphaMbeta2 integrin. *J Biol Chem*. 1996; 271(30):18211–18216.
43. Xiong YM, Chen J, Zhang L. Modulation of CD11b/CD18 adhesive activity by its extracellular, membrane-proximal regions. *J Immunol*. 2003; 171(2):1042–1050.
44. Li Y, Zhang L. The fourth blade within the beta -propeller is involved specifically in C3bi recognition by integrin alpha Mbeta 2. *J Biol Chem*. 2003; 278(36):34395–34402.
45. Cao C, et al. Endocytic receptor LRP together with tPA and PAI-1 coordinates Mac-1-dependent macrophage migration. *EMBO J*. 2006;25(9):1860–1870.